Magnetotransport studies of SiGe-based p-type heterostructures: Problems with the determination of effective mass

I. B. Berkutov, V. V. Andrievskii, Yu. F. Komnik, Yu. A. Kolesnichenko, R. J. H. Morris et al.

Citation: Low Temp. Phys. **38**, 1145 (2012); doi: 10.1063/1.4770520
View online: http://dx.doi.org/10.1063/1.4770520
View Table of Contents: http://ltp.aip.org/resource/1/LTPHEG/v38/i12
Published by the American Institute of Physics.

QUANTUM EFFECTS IN SEMICONDUCTORS AND DIELECTRICS

Magnetotransport studies of SiGe-based *p*-type heterostructures: Problems with the determination of effective mass

I. B. Berkutov,[a] V. V. Andrievskii, Yu. F. Komnik, and Yu. A. Kolesnichenko

B. Verkin Institute for Low Temperature Physics and Engineering, National Academy of Sciences of Ukraine, 47 Lenin Ave., Kharkov 61103, Ukraine

R. J. H. Morris and D. R. Leadley

Department of Physics, University of Warwick, Coventry CV4 7AL, United Kingdom

O. A. Mironov

International Laboratory of High Magnetic Fields and Low Temperatures, 95 Gajowicka, Wroclaw 53-24, Poland

(Submitted June 5, 2012)
Fiz. Nizk. Temp. **38**, 1455–1463 (December 2012)

The use of Shubnikov-de Haas oscillations for determining effective mass is illustrated by a study of the magnetotransport properties of the two-dimensional hole gas in $Si_{1-x}Ge_x$ ($x = 0.13$, 0.36, 0.95, 0.98) quantum wells. For some samples the data cannot be fitted to standard theoretical curves in which the scattering of charge carriers is described by the conventional Dingle factor. The reasons for the discrepancies between the experiment the theory are: (i) the effect of spin splitting on the amplitude of the peak in the SdH oscillations; (ii) extra broadening of the Landau levels attributable to an inhomogeneous distribution of the carrier concentration; (iii) the coexistence of short and long-range scattering potentials; and, (iv) population of the second energy level in the quantum well. Ways of calculating the effective hole masses m^* for all these cases are presented and values of m^* are found for the heterostructures studied here. © *2012 American Institute of Physics*. [http://dx.doi.org/10.1063/1.4770520]

1. Introduction

One advantage of band engineering in SiGe heterostructures is the ability of enhance the mobility of the charge carriers. In particular, the enhancement of hole mobility is desirable in Si/SiGe-based materials since *p*-type devices limit the performance of complementary MOS type circuits because of their intrinsically lower mobility. Among various types of SiGe heterostuctures designed to increase hole mobility μ_H, strained and high content Ge channel modulation-doped structures have provided the highest mobility both at low temperatures, where $\mu_H = 120 \times 10^3$ cm^2/(V·s) at 2 K with a carrier density of 8.5×10^{11} cm^{-2},[1] and at room temperature, where $\mu_H = 3.1 \times 10^3$ cm^2/(V·s) with a carrier density of 4.1×10^{12} cm^{-2}.[2] This mobility increase comes primarily from the fact that the effective hole mass decreases with increasing Ge content.[3]

The effective mass m^* of the charge carriers is an important parameter in determining the kinetic and thermodynamic properties of a conducting system. For example, if m^* is known, then the isotropic two-dimensional (2D) density of states for a gas of noninteracting carriers is given by $n_{2D} = m^*/(\pi\hbar^2)$. m^* of 2D charge carriers can be measured using quantum cyclotron resonance (CR)[4] or Shubnikov-de Haas (SdH) oscillations.[5] Both methods use a magnetic field to create Landau levels within the material. In the quantum cyclotron resonance method, the transition energy between Landau levels is measured directly, but this method is limited by strict specifications on the experimental conditions and the material under examination. The effective mass can also be found from the temperature dependence of the amplitude of SdH oscillations. This method introduces some averaging, but typically works at lower fields than those used in CR experiments and it is a purely electrical transport measurement. The relative simplicity of SdH experiments is the reason that a majority of effective masses have been measured in this way. This paper is a study of the effective mass of $Si_{1-x}Ge_x$ ($x = 0.13$, 0.36, 0.95, 0.98) *p*-type quantum wells (QWs) using the SdH technique. A number of deviations from the ideal theoretical model show up in the data owing to structural features of the quantum wells and the technology used to prepare them and will be discussed below.

2. Structure of the samples

All the heterostructures studied here have been designed to have a two-dimensional hole gas (2DHG) in a biaxial compressive strained $Si_{1-x}Ge_x$ alloy channel. Three of the heterostructures were grown by the molecular beam epitaxy (MBE) and are labelled samples "A," "B," and "C," with quantum wells in $Si_{0.87}Ge_{0.13}$, $Si_{0.64}Ge_{0.36}$, and $Si_{0.05}Ge_{0.95}$ channels, respectively. The detailed MBE growth conditions are as follows. Heterostructure "A" has a 35 nm thick QW of $Si_{0.87}Ge_{0.13}$ grown pseudomorphically at 870 °C on a Si (001) substrate and is remotely doped from above the QW with 2×10^{18} cm^{-3} of boron in a 50 nm Si layer grown at 750 °C.[6] Heterostructure "B" is similar with a 10 nm thick pseudomorphic QW of $Si_{0.64}Ge_{0.36}$ grown at 450 °C and

annealed *in situ* at 800 °C before completing the structure with remote B-doping above the QW with 2×10^{18} cm^{-3} of boron in a 50 nm Si layer grown at 600 °C.[7] This kind of low-temperature QW growth and *in situ* annealing was used to avoid the growth-induced roughening of the top $Si_{0.64}Ge_{0.36}$/Si interface typically observed for growth temperatures above 550 °C and leads to dramatically reduced 2DHG mobility in the QW for $T < 10$ K.

Sample "C" was metamorphic, with an intermediate relaxed $Si_{0.4}Ge_{0.6}$ buffer grown on the Si (001) substrate followed by a strained $Si_{0.05}Ge_{0.95}$ QW. In this sample boron doping was introduced both on top and underneath the QW, with MBE growth conditions similar to those in Ref. 8; however, for sample "C" the doping was asymmetric with the boron-doped $Si_{0.4}Ge_{0.6}$ layers having concentrations of 2×10^{18} and 8×10^{18} cm^{-3}, respectively, below and above the QW.

The metamorphic sample "D" Si/$Si_{0.4}Ge_{0.6}$/$Si_{0.02}Ge_{0.98}$/$Si_{0.4}Ge_{0.6}$ was grown by a hybrid-epitaxy technique that used UHV-CVD for the virtual substrate and SS-MBE for the active heterostructure, consisting of a 20 nm $Si_{0.02}Ge_{0.98}$ QW grown at 350 °C with remote/inverted B-doping to 3.6×10^{18} cm^{-3}.[9] Sample "D" was also annealed *ex situ* at 650 °C as this had been previously found to yield the highest 2DHG mobility for this type of sample, 22 100 cm^2/(V·s) at 10 K. The strained QW for sample "D" was meant to be "technologically pure Ge,"[9] but high resolution XRD and SIMS measurements after growth and annealing by revealed it to be ~98% Ge.[10]

Conventional Hall bar geometries were found for all the samples. For samples "A," "C," and "D," the diagonal $\rho_{xx}(B)$ and off-diagonal $\rho_{xy}(B)$ components of the resistance tensor were measured up to 11 T, while for sample "B" it was only measured up to 6 T. The measurements were performed using a standard lock-in technique at a frequency of 33 Hz and a current of 10 nA for samples "A," "B," and "C," and 100 nA for sample "D". No overheating effects were observed at these current levels. The lowest measurement temperatures for the samples were: 33 mK for sample "A," 350 mK for samples "B" and "C," and 1.45 K for sample "D." The measured $\rho_{xx}(B)$ and $\rho_{xy}(B)$ curves for these temperatures are shown in Fig. 1 (where $\rho_{xx}(B)$ represents the resistance per square area of the 2DHG). These curves exhibit pronounced Shubnikov-de Haas oscillations for $B \geq 1$ T and steps representative of the quantum Hall effect plateaux are observed for sample "A." The 2DHG parameters found from the measurement of resistance, Hall effect and Shubnikov- de-Haas oscillations at these temperatures are listed in Table 1.

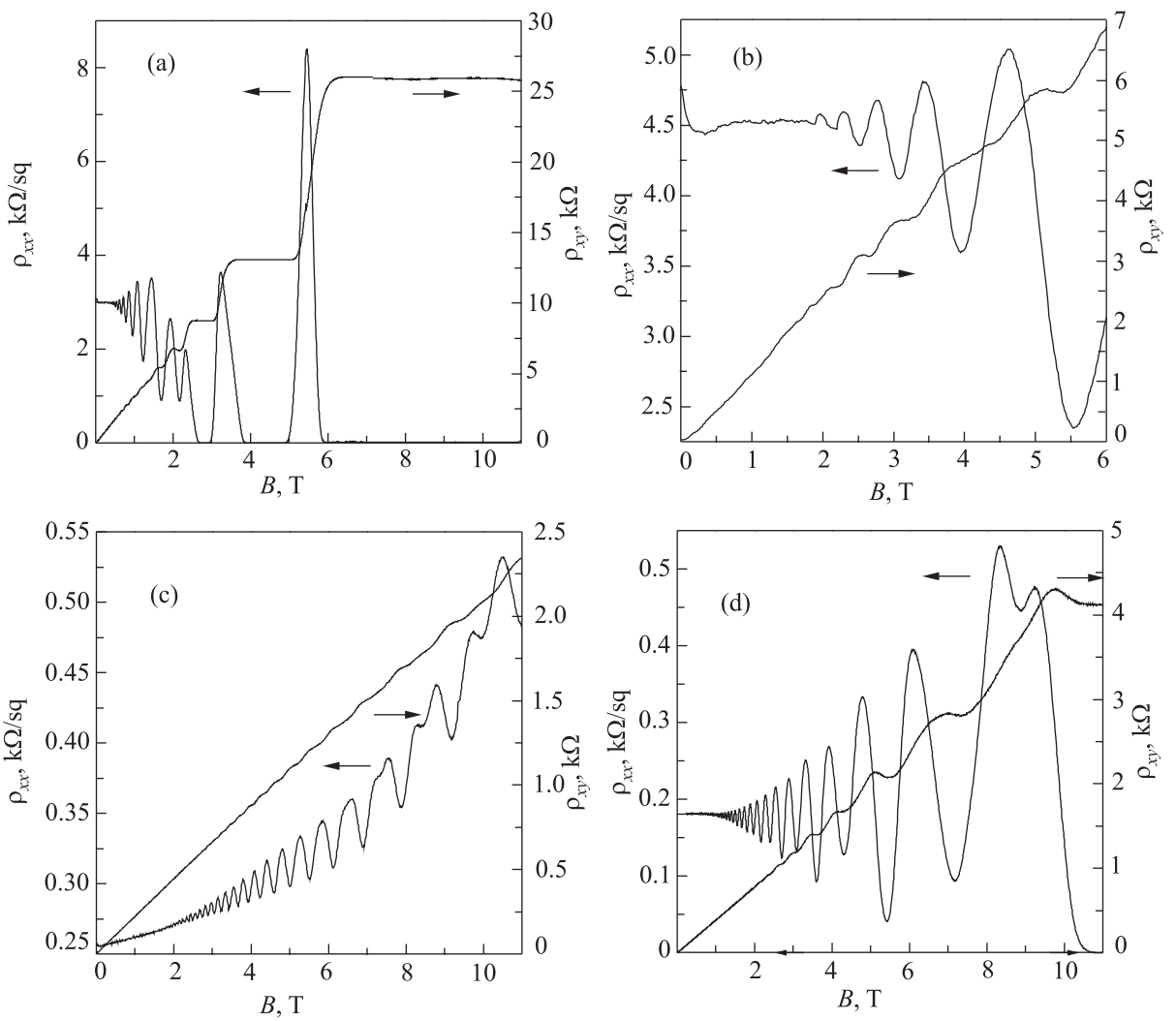

FIG. 1. Magnetoresistance ρ_{xx} and ρ_{xy} of samples "A" (a) at $T = 33$ mK, "B" (b) at 350 mK, "C" (c) at 350 mK, and "D" (d) at $T = 1.45$ K.

TABLE 1. Parameters of 2DHG in strained and remotely doped SiGe QWs.

Sample	Quantum channel	ρ_{xx},kΩ	p_{Hall}, cm^{-2}	p_{SdH}, cm^{-2}	μ_{Hall}, cm^2/(V·s)	m,m_0	α
A	$Si_{0.87}Ge_{0.13}$	3.04	1.9×10^{11}	2.1×10^{11}	1.17×10^4	0.21 ± 0.03	1.02
B	$Si_{0.64}Ge_{0.36}$	4.78	6.42×10^{11}	6.7×10^{11}	0.22×10^4	0.24 ± 0.005	1.05
C	$Si_{0.05}Ge_{0.95}$	0.247	2.82×10^{11}	2.98×10^{12}	0.91×10^4	0.17 ± 0.01	4.4
D	$Si_{0.02}Ge_{0.98}$	0.16	1.62×10^{11}	0.95×10^{12}	2.21×10^4	0.12 ± 0.005	8.6
				0.68×10^{12}			20

3. Determination of *m**

The effective mass m^* and quantum scattering time of the charged particles, which leads to the broadening of the Landau levels, are usually estimated from the temperature and magnetic field dependent SdH oscillation amplitude (ΔR). ΔR is the deviation of the adjacent maximum and minimum of the resistance from the averaged monotonic resistance R_0 and is a function of magnetic field B. The change in resistivity (i.e., conductivity) of the 2D gas is a quantum effect and is considered theoretically in Refs. 11 and 12. Assuming homogeneous broadening of the Landau levels, the modulation of the electrical resistance is[12]

$$\rho_{xx}(B) = \rho_0^{-1} \times \left[1 + 4\sum_{s=1}^{\infty}\left(\frac{\Psi s}{\sinh\Psi s}\right) \times \exp\left(-\frac{\pi s}{\omega_c \tau_q}\right)\cos\left(\frac{2\pi s \varepsilon_F}{\hbar\omega_c} - s\pi\right)\right], \qquad (1)$$

where $\Psi = 2\pi 2kBT\ /(\hbar\omega_c)$ determines the temperature and magnetic field dependences of the amplitude of the oscillations and $\omega_c = eB/m^*$ is the cyclotron frequency. The Fermi energy for the 2D case is given by $\varepsilon_F = \pi\hbar^2 n/m^*$, where n is the concentration of charge carriers. In practice, the sum (s) in Eq. (1) can be taken to be 1, i.e., $s = 1$, which is correct if $\omega_c\tau_q \ll 1$ as in the case of our samples. The second factor in the sum (called the Dingle factor) describes homogeneous broadening in the Landau levels due to a finite quantum state lifetime τ_q. It should be noted that this lifetime differs[13] from the Drude transport lifetime τ which defines the conductivity $\sigma = ne^2\tau/m^*$. We found that τ for our samples is almost independent of temperature and magnetic field within the ranges studied here. We assume that τ_q is also independent of magnetic field and temperature, so it is not involved in the following analysis. Finally, the first term in the sum describes the damping of the SdH oscillations caused by temperature broadening of the Fermi function.

The mass and concentration of carriers can be found from the period and amplitude of SdH oscillations (at different temperatures) as a function of inverse magnetic field by plotting $\ln[(\Delta R/R_0)(\sinh\Psi)/\Psi]$ as a function of $1/(\omega_c\tau)$ or $1/(\mu B)$, where μ is the carrier mobility (Dingle plot). The argument of the exponential term in Eq. (1) can now be rewritten as $-\pi\alpha/(\omega_c\tau)$, $\alpha = \tau/\tau_q$. According to Eq. (1), plotting the points corresponding to the extrema with different numbers ν of Landau levels should result in a straight line with a slope proportional to $\pi\alpha$. Then the effective mass m^* becomes the fitting parameter.[14] According to Eq. (1), for an extremely strong magnetic field $(1/\omega_c\tau \to 0)$ $(\sinh\Psi)/\Psi \to 1$, so this straight line should bisect the $\ln[(\Delta R/R_0)(\sinh\Psi)/\Psi]$ axis at $\ln 4 \approx 1.386$. Furthermore, the experimental data for a plot of $\ln[\Delta R/R_0]$ vs $\ln(\Psi_s/\sinh\Psi_s) - \pi\alpha/(\omega_c\tau)$, which can be used to find α as a fitting parameter, should also result in a straight line with a gradient equal to unity.[14]

However, it turns out that in many cases the experimental data could not be exactly fitted by a single straight line for all magnetic fields, but instead deviates from that at small values of the arguments and has different intercepts.

An example of the method described above for determining m^* is shown in Fig. 2 for sample "B." From this analysis m^* was estimated to be 0.24 m_0 (where m_0 is free electron mass) and $\alpha = 1.05$. The solid line on Fig. 2 is the straight line predicted by Eq. (1) with an intercept at ln 4 which is as good fit to the experimental data. Figures 3–5 show similar plots for the other samples; these manifest a number of deviations from the dependence predicted by

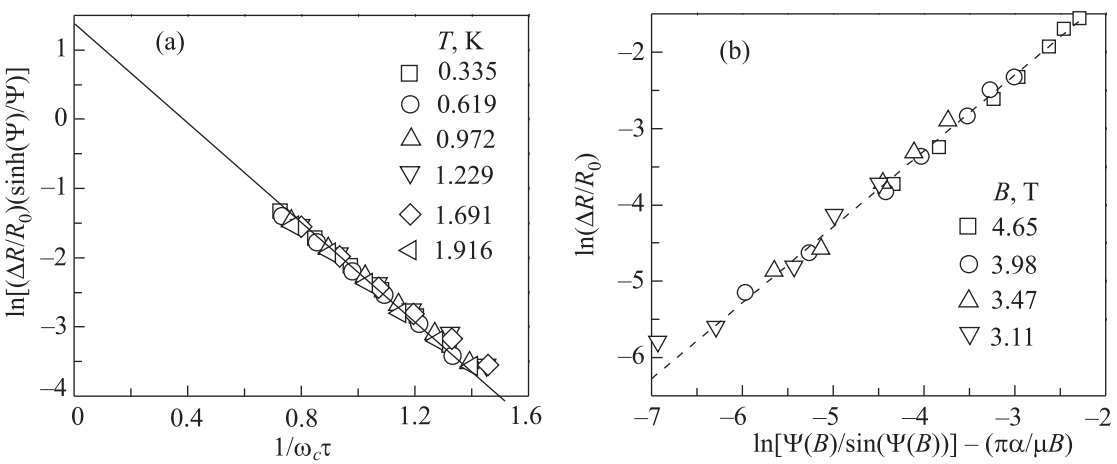

FIG. 2. Plots for self-consistent determination of the effective mass m^* and the parameter α for sample "B" at different temperatures (a) and magnetic fields (b).

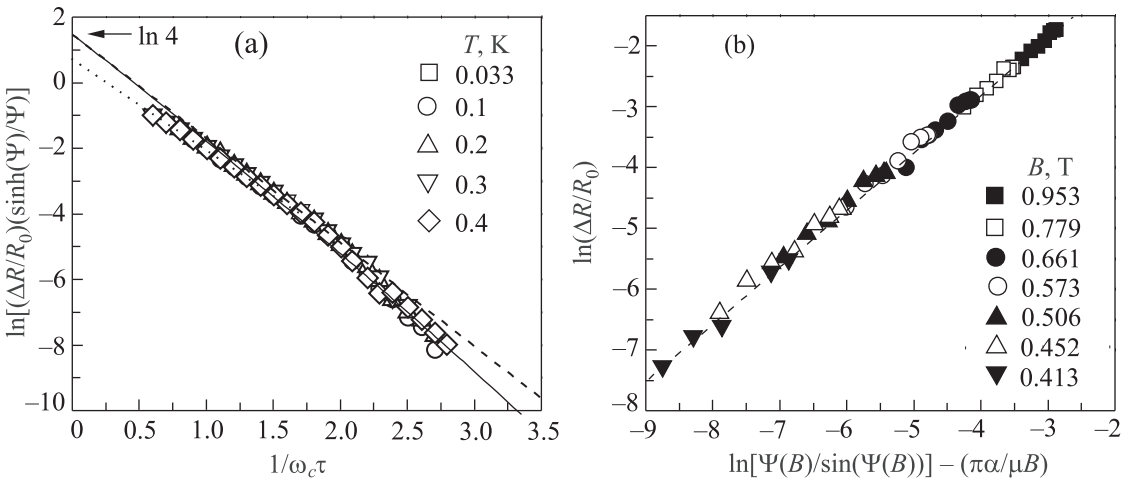

FIG. 3. Plots for self-consistent determination of the effective mass m^* and the parameter α for sample "A" at different temperatures (a) (solid line is theory[12]) and magnetic fields (b). The dashed line is a guide for the eye.

Eq. (1), both quantitatively and qualitatively, and are typical of the deviations seen in many previous reports. In the following discussion below, we show how these deviations may be related to structural features of the QWs and the technology used in their preparation.

4. Deviations from the theory

4.1. Influence of Zeeman spin splitting

In the Dingle plot of Fig. 2(a) for sample "B," the data for weak magnetic fields in the limit $1/\omega_c\tau \to 0$ lie on a straight line with an intercept at ln 4. However, for strong magnetic fields ($1/\omega_c\tau < 1.3$) a small downward deviation is observed. This is because the amplitude of the SdH oscillations is less than expected in the theory, owing to spin (Zeeman) splitting affecting the maxima, and changes in the SdH oscillation shape as the resistivity approaches zero at the minima (see Fig. 1(a)). In the limit of strong magnetic fields the spin splitting obviously splits the maxima of the SdH oscillations and these extremes are clearly not included in the m^* calculation; however, for intermediate magnetic fields the spin splitting may not be fully resolved, but can still cause a drop in the observed the oscillation amplitude and lead to a deviation from the theory.[12]

4.2. Extra "inhomogeneous broadening" of the Landau levels

Attention has been drawn to a nonlinearity in the ln $[(\Delta R/R0)(\sinh\Psi)/\Psi]$ vs $1/(\omega_c\tau)$ dependence in high-mobility systems in Refs. 15 and 16, for instance. At low magnetic fields the reason for the deviation from the theory is as follows: it is assumed[16] that in some cases (mainly in high-mobility systems with a 2D gas of charge carriers) the nonlinearity is caused by spatial variations (in the 2D gas plane) in the electron concentration and hence in the Fermi energy. Thus, the oscillation extrema in different parts of the sample occur at slightly different magnetic fields, so that the total oscillation amplitude is lower than for a homogeneous sample. This leads to an additional effective broadening of the Landau levels (so-called "inhomogeneous broadening").[16]

The formation of the SdH oscillations in the case of long-range fluctuations (i.e., in the plane of a 2D gas) in the potential, electron concentration, and Fermi energy are described by a Gaussian in Ref. 16. It was shown that an additional term $-[\pi\delta\varepsilon_F/(\hbar\omega_c)]^2$ appears in the argument of

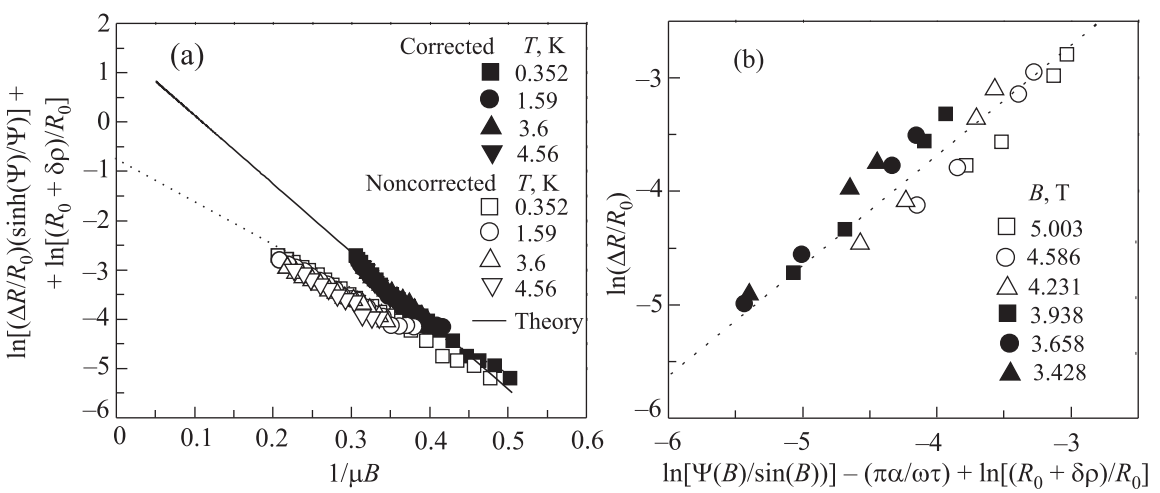

FIG. 4. Plots for self-consistent determination of the effective mass m^* and the parameter α for sample "C" at different temperatures (a) (hollow symbols indicate calculations with $\sigma_0^{-1} = \rho_0$ ($B = 0$) and the solid symbols, calculations taking the magnetic field dependence of the monotonic magnetoresistance background into account) and magnetic fields (b). The dashed line is a guide for the eye.

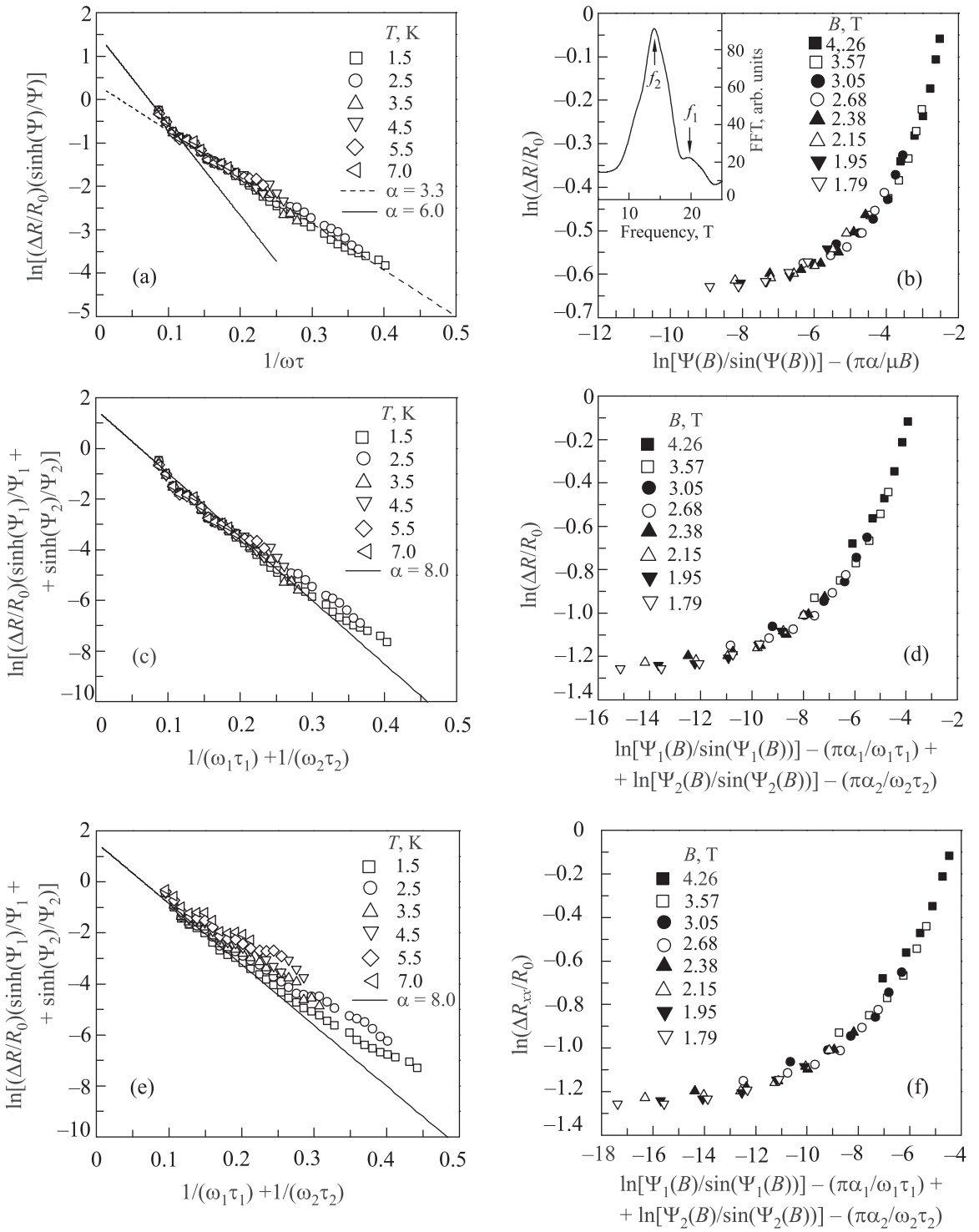

FIG. 5. Plots for self-consistent determination of the effective mass m^* and the parameter α for sample "D" at different temperatures and magnetic fields using the theoretical model of Ref. 12 for $m^* = 0.12m_0$ (a) and $\alpha = 8$ (b); with the existence of two levels of magnetic quantization taken into account for $m_1^* = m_2^* = 0.12m_0$ (c), $\alpha_1 = 8.6$, $\alpha_2 = 20$ (d), and $m_1^* = 0.12m_0$, $m_2^* = 0.147m_0$ (e), $\alpha_1 = 6.4$, $\alpha_2 = 24$ (f) calculated according to the theory of Ref. 21. The inset shows an FFT of the SdH oscillations at $T = 1.45$ K and indicates two periods.

the exponential in Eq. (1). The exponential factor in Eq. (1) therefore becomes

$$\exp\left[-\frac{\pi}{\omega_c\tau_q} - \left(\frac{\pi^2\hbar\delta n}{m^*\omega_c}\right)^2\right]. \qquad (2)$$

The first term in the exponent still describes collisional broadening of the Landau levels and is inversely proportional to the magnetic field. The second term now accounts for the "inhomogeneous broadening" of the Landau levels and is inversely proportional to the square of the field.

Figure 3(a) illustrates the possibility of describing the experimental dependences of $Y = \ln[(\Delta R/R_0)(\sinh\Psi)/\Psi]$ on $X = 1/(\omega_c\tau)$ by the polynomial $Y = -a_1X - a_2X^2 + \text{const}$ where, according to Eqs. (1) and (2), $a_1 = \pi\tau/\tau_q$ and $a_2 = (\pi^2\hbar\tau\delta p/m^*)^2$. In this approximation $m^* = (0.21 \pm 0.03)m_0$ and $\alpha = 1.02$ are found from the linear term (dashed line in Fig. 3(a)) and $\delta p = 4 \times 10^9\,\text{cm}^{-2}$, or only 2% of $p_{SdH} = 2.1 \times 10^{11}\,\text{cm}^{-2}$, from the quadratic term.[17]

4.3. Large positive quasiclassical magnetoresistance

For sample "C" the above procedure was applied using the resistance in zero field ($\rho_0 \sim 1/\sigma_0$). The Dingle plot for all the experimental points results in a straight line (hollow symbols in Fig. 4(a)). However, extrapolation of this line to $1/\omega_c\tau \to 0$ (dashed line in Fig. 4(a)) does not give an intercept at ln 4. The reason for this difference from Eq. (1) is the presence of a large positive change against the monotonic background of the magnetoresistance (see Fig. 1(c)). This positive change is well described by the function $\rho_{xx}(B)/\rho_{xx}(0) \propto B^{12/7}$ as predicted by quasiclassical theory[18,19] with the combined influence of a short-range potential from the scattering centers in the quantum channel and the long-range potential from impurity atoms in the remote doping layers taken into account. This monotonic background causes a shift in the resistance at the minima and maxima in the SdH oscillations; it does not result from a constant ρ_0, but from the values $\rho_B = \rho_0 + \Delta\rho(B)$ which are determined by the change in the monotonic background from the magnetoresistance. To include this monotonic background, the calculations with Eq. (1) were done using ρ_B instead of ρ_0. Therefore, the dependence of $\ln[(\Delta R/R_0)(\sinh\Psi)/\Psi] + \ln[\rho B(B)/\rho_0]$ on $1/(\mu B)$ (up to a constant term) should be used instead of the dependence of $\ln[(\Delta R/R_0)(\sinh\Psi)/\Psi]$ on $1/(\mu B)$ to obtain the abscissa in Fig. 4(a). The solid points in Fig. 4(a) indicate the experimental data and the solid corresponds to the theory of Ref. 12 and yields ln 4 as $1/(\omega_c\tau) \to 0$. Based on this, appropriate adjustments were made in the curves of Fig. 4(b). The estimated effective mass of sample "C" is $m^* = 0.17m_0$ and $\alpha = 4.4$.

4.4. 2D systems with two populated subbands

The results of the calculations for sample "D" according to the theory of Ref. 12 are shown in Fig. 5. The experimental curve (Fig. 5(a)) is highly nonlinear and has a kink at $B \sim 3.5$ T, and for this value one of the curves in Fig. 5(a) can be obtained with $m^* = 0.12\,m_0$. However, two values of α are found. For strong magnetic fields, i.e., before the kink in Fig. 5(a)), a value of $\alpha = 3.3$ is found. At lower magnetic fields this value is approximately $\alpha = 6$. The experimental curve in Fig. 5(b) is also highly nonlinear, but the data points for different magnetic fields can be arranged on a single curve by taking $\alpha = 8$. Fast Fourier transform analysis of the oscillatory part of $\rho_{xx}(B)$ (see inset in Fig. 5(b)) revealed the presence of two maxima. From these data and the effect of "beating" observed in the SdH oscillations (see Fig. 1(d)), we conclude that two populated hole subbands exist, so there are two sets of SdH oscillations. The frequencies $f_1 = 19.5$ T and $f_2 = 14$ T are found and correspond to first and second subbands with hole concentrations $p_1 = 2ef_1/h = 0.95 \times 10^{12}\,\mathrm{cm}^{-2}$ and $p_2 = 2ef_2/h = 0.68 \times 10^{12}\,\mathrm{cm}^{-2}$, respectively. At the same time, the sum of these values, i.e., $p_1 + p_2$, yields a concentration within 1% of that obtained from Hall measurements. Thus, we conclude that the simple theoretical model[12] does not apply to this case. Early models that describe the magnetoresistance of 2D systems in the presence of two populated subbands[20,21] do not give a successful description of the experimental results and the theory of Ref. 21 is inapplicable here because the magnetic quantized subbands are not completely filled. The most successful description of our data is obtained by using the theoretical model of Refs. 23 and 24, where the resistance of the 2D system is given by[24]

$$\rho = \rho^{(0)} + \rho^{(1)} + \rho^{(2)}, \tag{3}$$

where $\rho^{(0)}$ is the classical resistance, $\rho^{(1)}$ is the first-order quantum correction describing the SdH oscillations, and $\rho^{(2)}$ is the second-order quantum contribution. The classical resistance is

$$\rho^{(0)} = \frac{m^*}{e^2 p_s}\frac{\omega_c^2 \upsilon_s + \upsilon_0 \upsilon_r^2}{\omega_c^2 + \upsilon_r^2}. \tag{4}$$

Here $p_s = p_1 + p_2$ is total density of charge carriers and ω_c is the cyclotron frequency, The characteristic rates υ_s, υ_r, and υ_0 are given by

$$\upsilon_s = \left(\frac{p_1}{p_s}\right)\upsilon_{11}^{\mathrm{tr}} + \left(\frac{p_2}{p_s}\right)\upsilon_{22}^{\mathrm{tr}} + \upsilon_{12}^{\mathrm{tr}},$$

$$\upsilon_r = \left(\frac{p_2}{p_s}\right)\upsilon_{11}^{\mathrm{tr}} + \left(\frac{p_1}{p_s}\right)\upsilon_{22}^{\mathrm{tr}} + 2\upsilon_{12} - \upsilon_{12}^{\mathrm{tr}},$$

$$\upsilon_0 = \frac{D}{\upsilon_r}, \quad D = (\upsilon_{11}^{\mathrm{tr}} + \upsilon_{12})(\upsilon_{22}^{\mathrm{tr}} + \upsilon_{12}) - \frac{(\upsilon_{12} - \upsilon_{12}^{\mathrm{tr}})^2 p_s^2}{4p_1p_2},$$

where the υ_{ij} are the elastic quantum scattering rates in the absence of a magnetic field and the υ_{ij}^{tr} are transport rates for intrasubband scattering. The first-order quantum contribution is[24]

$$\rho^{(1)} = -I\frac{2m^*}{e^2 p_s}\sum_{j=1,2}\left[\frac{2p_j}{p_s}\upsilon_{jj}^{\mathrm{tr}} + \upsilon_{12}^{\mathrm{tr}}\right]\exp(-\alpha_j)\cos\frac{2\pi(\varepsilon_F - \varepsilon_j)}{\hbar\omega_c}, \tag{5}$$

where $\alpha_j = \pi\upsilon_j/\omega_c$, $\upsilon_j = \upsilon_{jj} + \upsilon_{12}$, the ε_j are the subband energies, and $I = \Psi/\sinh\Psi$ with $\Psi = 2\pi^2 T/\hbar\omega_c$. The second order quantum contribution, which describes both the positive magnetoresistance and the magneto-intersubband (MIS) oscillations,[25] whose maxima correspond to integral ratios of the subband splitting energy $\Delta_{12} = \varepsilon_2 - \varepsilon_1$ to the cyclotron energy $\hbar\omega_c$,[24] is given by

$$\rho^{(2)} = \frac{2m^*}{e^2 p_s}\left[\frac{p_1}{p_s}\upsilon_{11}^{\mathrm{tr}}\mathrm{e}^{-2\alpha_1} + \frac{p_2}{p_s}\upsilon_{22}^{\mathrm{tr}}\mathrm{e}^{-2\alpha_2} + \upsilon_{12}^{\mathrm{tr}}\mathrm{e}^{-\alpha_1-\alpha_2}\cos\frac{2\pi\Delta_{12}}{\hbar\omega_c}\right]. \tag{6}$$

The results of the models given in Refs. 23 and 24 are shown in Fig. 6(a). The following kinetic characteristics of the sample were determined: effective mass $m^* = 0.12m_0$; α at the two subbands is $\alpha_1 = 8.6$ and $\alpha_2 = 20$; $\Delta_{12} = 18.7$ meV; and, $\nu_{12} = 4 \times 10^{11}\,\mathrm{s}^{-1}$. A simple accounting for the existence of the two subbands in the models analogous to those for other samples (see Figs. 5(c) and 5(d)) showed that the experimental points form a monotonic curve when the parameters found according to the theory of Refs. 23 and 24 are used (this model does not include the second-order quantum contribution and applies when the latter is small).

It has been shown[10] that for a similar structure to that of the sample "D" two different values of the effective mass $m_1^* = 0.12m_0$ and $m_2^* = 0.147m_0$ could be expected based

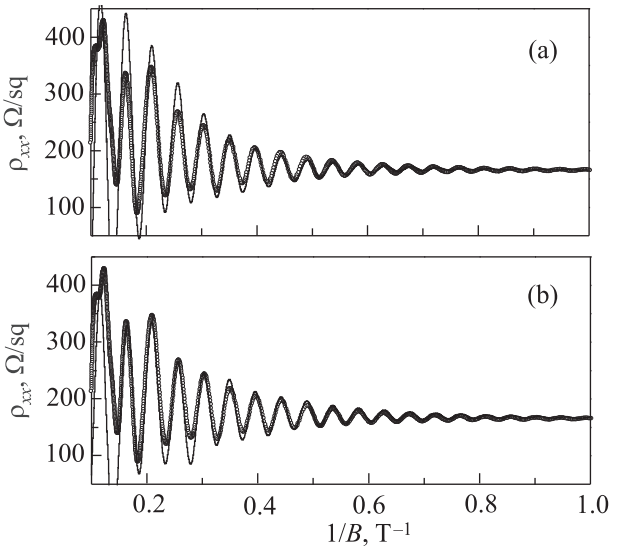

FIG. 6. The magnetoresistance ρ_{xx} of sample "D" as a function of the reciprocal of the magnetic field (hollow symbols). The solid curves are given by the theory of Refs. 23 and 24 for the cases $m_1^* = m_2^* = 0.12m_0$ (a) and $m_1^* = 0.12m_0$, $m_2^* = 0.147m_0$ (b).

on 4×4 Luttinger Hamiltonian calculations (for the simplified case of a rectangular QW). At low magnetic fields $B \sim 5$ T, only one broad CR line was observed with an effective cyclotron mass of $m_1^* = 0.12m_0$, which coincides with the calculated CR effective mass in the first electric subband. The width of the CR line has been explained in terms of CR transitions from these two subbands at different fields, which results in significant CR line broadening.[10] Two different values of m^* were also reported in Ref. 26, where it was shown that the lowest hole bound state in the surface potential well at a GaAs-(AlGa)As heterojunction interface consists of two subbands, which are degenerate for $k = 0$. The lifting of the spin degeneracy for $k \neq 0$ owing to a lack of inversion symmetry at the heterojunction interface gives rise to two cyclotron masses: $m_1^* = 0.36m_0$ and $m_2^* = 0.6m_0$.

This possibility was further explored by using the above values of the effective mass. Results from experimental studies of the inverse magnetic field dependence of the resistance in the framework of the theory of Refs. 23 and 24 are shown in Fig. 6(b). A comparison of the data in Figs. 6(a) and 6(b) reveals no significant difference. At the same time, a simple accounting for the existence of two different values of m^* on different subbands (see Figs. 5(e) and 5(f)) showed that the experimental points are not from a single monotonic curve.

For a more precise statement, further study using the cyclotron resonance method will be necessary.

5. Conclusion

In this work the 2DHG effective mass m^* for a different Ge concentrations in SiGe QW structures has been determined on the basis of Shubnikov-de Haas oscillations. The deviation of our experimental data from a theory for SdH-related conductivity oscillations[12] can be explained by the following:

— Spin splitting of the peaks in the SdH oscillations, which results in a decrease in the amplitudes of the oscillations;
— Extra broadening of the Landau levels which is attributed to the existence of a 2% inhomogeneous distribution in the carrier concentration of the 2D charge layer and, therefore, in their energy. It is believed that the extra broadening is from the natural variation of the well width on an interatomic distance scale:[16]
— Observation of both SdH oscillations and a large, nonsaturating positive quasiclassical magnetoresistance which is a consequence of the short and long-range scattering potentials as predicted by the theory.[18]

In the case where more than one quantized subband is filled, it is no longer possible to analyze the SdH oscillations using the simple model of Ref. 12. In that case, a more detailed analysis is necessary.

We thank T. Hackbarth (Daimler AG Forschungszentrum, 89081 Ulm, Germany), for MBE growth/fabrication of sample "C." Measurements were made at the Nanosilicon Group, Department of Physics, University of Warwick, Coventry, UK, and, partially, at the International Laboratory of High Magnetic Fields and Low Temperatures, Wroclaw, Poland.

[a]Email: berkutov@ilt.kharkov.ua

[1]B. Rössner, D. Chrastina, G. Isella, and H. von Känel, Appl. Phys. Lett. **84**, 3058 (2004).
[2]M. Myronov, K. Sawano, Y. Shiraki, T. Mouri, and K. M. Itoh, Appl. Phys. Lett. **91**, 082108 (2007).
[3]J. B. Roldán and F. Gámiz, Solid-State Electron. **48**, 1347 (2004).
[4]I. M. Lifshits, Zh. Exp. Teor. Fiz. **40**, 1235 (1961).
[5]S. M. Sze, *Phys. Semicond. Devices* (Wiley, New York, 1981).
[6]T. E. Whall, D. W. Smith, A. D. Plews, R. A. Kubiak, P. J. Phillips, and E. H. C. Parker, Semicond. Sci. Technol. **8**, 615 (1993).
[7]T. J. Grasby, C. P. Parry, P. J. Phillips, B. M. McGregor, R. J. H. Morris, G. Braithwaite, T. E. Whall, E. H. C. Parker, R. Hammond, A. P. Knights, and P. G. Coleman, Appl. Phys. Lett. **74**, 1848 (1999).
[8]G. Höck, M. Glück, T. Hackbarth, H. J. Herzog, and E. Kohn, Thin Solid Films **336**, 141 (1998).
[9]R. J. H. Morris, T. J. Grasby, R. Hammond, M. Myronov, O. A. Mironov, D. R. Leadley, T. E. Whall, E. H. C. Parker, M. T. Currie, C. W. Leitz, and E. A. Fitzgerald, Semicond. Sci. Technol. **19**, L106 (2004).
[10]O. A. Mironov, M. Goiran, J. Galibert, D. V. Kozlov, A. V. Ikonnikov, K. E. Spirin, V. I. Gavrilenko, G. Isella, M. Kummer, H. von Känel, O. Drachenko, M. Helm, J. Wosnitza, R. J. H. Morris, and D. R. Leadley, J. Low Temp. Phys. **159**, 216 (2010).
[11]T. Ando, J. Phys. Soc. Jpn. **37**, 1233 (1974).
[12]A. Isihara and L. Smrčka, J. Phys. C **19**, 6777 (1986).
[13]P. T. Coleridge, R. Stoner, and R. Fletcher, Phys. Rev. B **39**, 1120 (1989).
[14]T. E. Whall, N. L. Mattey, A. D. Plews, P. J. Phillips, O. A. Mironov, R. J. Nicholas, and M. J. Kearney, Appl. Phys. Lett. **64**, 357 (1994); T. E. Whall, A. D. Plews, N. L. Mattey, and E. H. C. Parker, Appl. Phys. Lett. **65**, 3362 (1994).
[15]J. P. Harring, R. J. Higgins, R. K. Goodall, P. R. Lay, M. Laviron, and P. Delesduse, Phys. Rev. B **32**, 8126 (1985).
[16]S. D. Bystrov, A. M. Kreshchuk, L. Tuan, S. V. Novikov, T. A. Polyanskaya, I. G. Saveliev, and A. Ya. Shik, Fiz. Tekh. Poluprovodu. **28**, 91 (1994).
[17]I. B. Berkutov, V. V. Andrievskii, Yu. F. Komnik, O. A. Mironov, M. Myronov, and D. R. Leadley, Fiz. Nizk. Temp. **35**, 188 (2009) [Low Temp. Phys. **35**, 141 (2009)].
[18]D. G. Polyakov, F. Evers, and P. Wölfle, Phys. Rev. B **64**, 205306 (2004).
[19]I. B. Berkutov, V. V. Andrievskii, Yu. F. Komnik, and O. A. Mironov, Fiz. Nizk. Temp. **36**, 1335 (2010) [Low Temp. Phys. **36**, 1076 (2010)].
[20]D. R. Leadley, R. Fletcher, R. J. Nicholas, F. Tao, C. T. Foxon, and J. J. Harris, Phys. Rev. B **46**, 12439 (1992).
[21]T. H. Sander, S. N. Holmes, J. J. Harris, D. K. Maude, and J. C. Portal, Phys. Rev. B **58**, 13856 (1998).
[22]M. E. Raikh and T. V. Shahbazyan, Phys. Rev. B **49**, 5531 (1994).

[23]O. E. Raichev, Phys. Rev. B **78**, 125304 (2008).
[24]N. C. Mamami, G. M. Gusev, E. C. F. da Silva, O. E. Raichev, A. A. Quivy, and A. K. Bakarov, Phys. Rev. B **80**, 085304 (2009).
[25]N. C. Mamani, G. M. Gusev, T. E. Lamas, A. K. Bakarov, and O. E. Raichev, Phys. Rev. B **77**, 205327 (2008).
[26]H. L. Stormer, Z. Schlesinger, A. Chang, D. C. Tsui, A. C. Gossard, and W. Wiegmann, Phys. Rev. Lett. **51**, 126 (1983).

This article was published in English in the original Russian journal. Reproduced here with stylistic changes by AIP.